

This would be expected if, because of suppressed diffusion, it were difficult for the  $F$  centers to escape from the strain fields of dislocations at which they were formed. If this hypothesis is correct, warmup to room temperature after irradiation should cause the  $F$  band to return to its normal width. As shown in Fig. 6, the  $F$  band does appear to narrow during a room-temperature anneal in a manner compatible with the above discussion. It is possible, however, that subsidiary absorption bands, which lie beneath the  $F$  band, contribute to the broadening and anneal at room temperature. It was also observed that a section of the same heavily deformed crystal, when x irradiated at room temperature, shows no excess  $F$ -band broadening.

### CONCLUSION

The optical absorption experiments performed at various temperatures agree with the prediction of the dislocation pinning model, developed from internal friction experiments, that edge dislocations always act as sites for vacancy formation during x irradiation. When the temperature is below that needed for diffusion of  $F$  centers, and the dislocation density is of the magnitude ordinarily present in rock salt, the dislocations are unable to enhance the optically observed  $F$ -center growth rate. The transition temperature between the passive and active role of dislocations in the generation of color centers falls at about 250°K for NaCl.

In general, the present experiments indicate that bulk

$F$  centers are formed at all temperatures either from vacancies already present or by a mechanism such as that proposed by Rabin and Klick. All aspects of the Rabin and Klick interstitial mechanism, which is the only effective source of additional vacancies at low temperatures, are compatible with the ideas presented here. However, as the temperature is increased the interstitial mechanism either stops or becomes relatively ineffective and the dislocation mechanism becomes active. The present experiments also emphasize a well-known but often overlooked fact: When  $F$  centers are located in the strain field produced by imperfections (mainly edge dislocations), they no longer retain the characteristic properties of  $F$  centers, i.e., their characteristic absorption band is displaced.

Mitchell, Wiegand, and Smoluchowski<sup>9</sup> have concluded from their analysis of the growth rate of  $F$  centers in crystals deformed up to 3% that the initial, deformation sensitive portion of the  $F$ -center growth curves is due to an additional concentration of vacancies created during the deformation process. If this were the correct description, it would be expected that the deformation contribution would be observed at all temperatures of irradiation. The present optical absorption measurements do not substantiate this type of behavior. A strong temperature dependence of the deformation contribution to  $F$ -center concentration is observed as shown in Fig. 3. This strongly suggests that the excess vacancies are formed during the irradiation.

## Interaction of Antiferromagnetic Spin Waves with a Bloch Wall\*

DAVID I. PAUL

*Physics Department, University of California, Los Angeles, California*

(Received November 13, 1961)

The interaction of an antiferromagnetic spin wave with a 180° Bloch wall is studied from the theoretical point of view. Our formulation includes the anisotropy and exchange energies of the crystal together with the characteristics of the wall such as its stiffness and viscosity. The anisotropy is assumed to be of a general orthorhombic form. We show that there exists a bound wall excitation branch as well as a free spin-wave excitation branch, and we derive a restrictive set of relationships between the excitations on two different sublattices. Further, we show that there exist special values of the energy for which the spin waves are degenerate and the restrictions no longer apply. Finally, we determine the change of phase of the spin waves on passing through the Bloch wall as a function of the wavelength, demonstrate that the phase change decreases as the wavelength increases, and compare our results with those of the analogous ferromagnetic case.

### I. INTRODUCTION

THE existence of antiferromagnetic domains has been experimentally demonstrated both by neutron and optical studies.<sup>1</sup> These domains usually arise from ordinary crystal imperfections such as dislocations,

grain boundaries, and crystallographic twins (see Fig. 1). Within these domains, it is possible to excite antiferromagnetic spin waves. It is the purpose of this paper to determine the effect of the domain wall on the transmission of antiferromagnetic spin waves from one domain to another. The analogous ferromagnetic case has been considered by Boutron<sup>2</sup> and by Winter.<sup>3</sup>

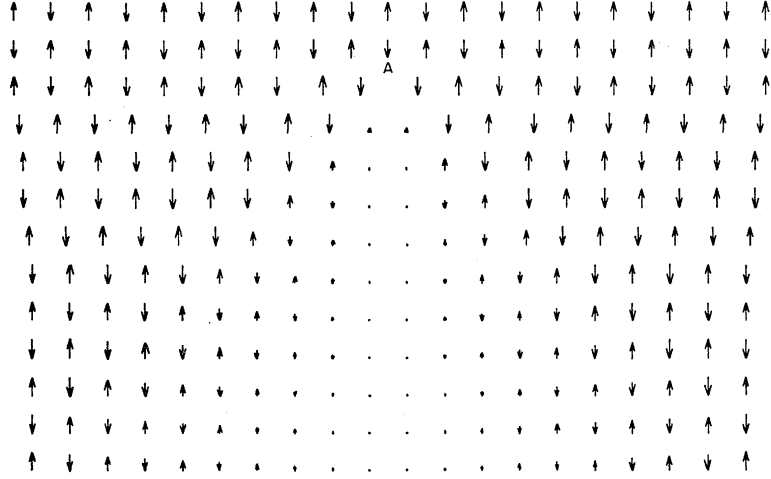
\* This research was supported in part by the Office of Naval Research.

<sup>1</sup> W. Roth, *J. Appl. Phys.* **31**, 2000 (1960).

<sup>2</sup> F. Boutron, *Compt. rend.* **252**, 3955 (1961).

<sup>3</sup> J. M. Winter, *Phys. Rev.* **124**, 452 (1961).

FIG. 1. Formation of a  $180^\circ$  Bloch wall by a dislocation at point A.



## II. FORMULATION OF THE PROBLEM

Consider an infinite antiferromagnetic crystal possessing orthorhombic type magnetic spin symmetry—the spins being located on two interpenetrating sublattices  $A$  and  $B$ . Each sublattice has six nearest neighbors all on the other sublattice. This situation is typical of many antiferromagnetic substances such as  $\text{CuCl}_2 \cdot 2\text{H}_2\text{O}$ . Further, we postulate the existence of a  $180^\circ$  Bloch wall dividing the crystal into two domains. Let the  $z$  axis be perpendicular to the wall with its zero point centered inside the wall (see Fig. 2). In the absence of a perturbation (i.e., spin wave), the magnetization vectors outside the wall are in the plus  $x$  direction on sublattice  $A$  and minus  $x$  direction on sublattice  $B$  for  $z$  less than zero and in the reverse direction for  $z$  greater than zero.

The Bloch walls separating the domains will have a finite thickness. We shall assume that the width of the wall is determined from minimum energy considerations between the magnetic anisotropy and exchange energies of the crystal—the angle between adjacent antiparallel spins changing slowly.<sup>4,5</sup> In a forthcoming paper we shall treat the case where the width of the domain wall is restricted to only a few atomic spaces by the lattice imperfections—this case requiring a different mathematical approach.

We write the anisotropy energy in the form

$$H_a = \sum_i [K_1(S_i^y)^2 + K_2(S_i^z)^2] + \sum_j [K_1(s_j^y)^2 + K_2(s_j^z)^2], \quad (1)$$

where  $S$  and  $s$  are the spin values of sublattice  $A$  and  $B$ , respectively. We shall let  $K_2$  be greater than  $K_1$ . Experimentally,<sup>6</sup> for  $\text{CuCl}_2 \cdot 6\text{H}_2\text{O}$ , the ratio  $K_2/K_1$  is

<sup>4</sup> C. Kittel and J. K. Gatt, in *Solid-State Physics*, edited by F. Seitz and D. Turnbull (Academic Press Inc., New York, 1956), Vol. 3.

<sup>5</sup> Y. Y. Li, *Phys. Rev.* **101**, 1450 (1956).

<sup>6</sup> R. Kubo, T. Nagamiya, K. Yosida, in *Advances in Physics*, edited by N. F. Mott (Taylor and Francis, Ltd., London, 1955), Vol. 4, p. 78.

equal to 3.3. Thus, within the Bloch wall, the spins will be parallel to the  $xy$  plane in order to minimize the anisotropy energy. Let  $\theta$  and  $\phi$  be the angles between the  $x$  axis and the static magnetization on sublattices  $A$  and  $B$ , respectively, and let us choose a new system of axes  $X$ ,  $Y$ , and  $z$ , where  $X$  is the spin direction for the static magnetization and  $X$  and  $Y$  vary from atom to atom while  $z$  is not changed. (See Fig. 2.) Then the anisotropy energy becomes

$$H_a = \sum_i \{ K_1[(S_Y^i)^2 \cos^2 \theta_i + (S_X^i)^2 \sin^2 \theta_i + 2S_X^i S_Y^i \cos \theta_i \sin \theta_i] + K_2(S_z^i)^2 \} + \sum_j \{ K_1[(s_Y^j)^2 \cos^2 \phi_j + (s_X^j)^2 \sin^2 \phi_j + 2s_X^j s_Y^j \cos \phi_j \sin \phi_j] + K_2(s_z^j)^2 \}. \quad (2)$$

We write the exchange part of the Hamiltonian in the form

$$H_{\text{ex}} = -2J \sum_{i,j} S_i s_j, \quad (3)$$

where the summation is over all pairs of nearest neighbors and  $J$  is negative. In our new coordinate system

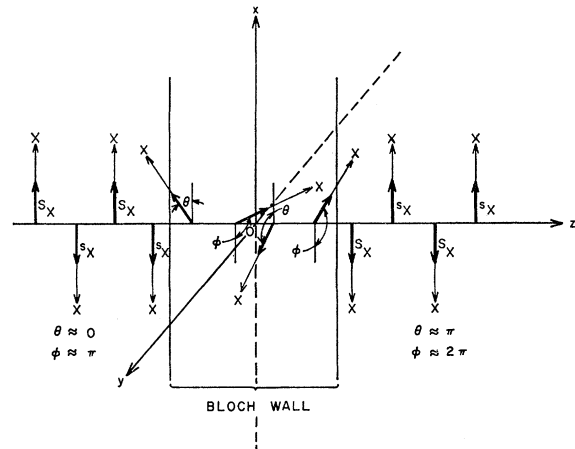


FIG. 2. Diagram showing fixed axis  $z$  perpendicular to Bloch wall, angles of deviation  $\theta$  and  $\phi$  of the different sublattice spins inside the wall, and varying coordinate axes,  $X$ .

this becomes

$$H_{\text{ex}} = -2J \sum_{i,j} S_z^i S_z^j - 2J \sum_{i,m} [\cos(\theta_i - \phi_{i+m}) \times (S_X^i S_X^{i+m} + S_Y^i S_Y^{i+m}) + \sin(\theta_i - \phi_{i+m}) \times (S_X^i S_Y^{i+m} - S_Y^i S_X^{i+m})] + 2J \sum_{i,l} (S_X^i S_X^{i+l} + S_Y^i S_Y^{i+l}), \quad (4)$$

where  $m$  and  $l$  are unit lattice vectors in the  $z$  direction and perpendicular to the  $z$  direction, respectively.

### III. STATIC CASE

Our unperturbed energy or ground state is determined by placing  $S_Y$ ,  $S_z$ ,  $s_Y$ , and  $s_z$  equal to zero,  $S_X$  and  $s_X$  equal to  $S$ , and minimizing the energy with respect to  $\theta$  and  $\phi$  where these angles are functions of  $z$  only. Thus, expanding  $\phi_j$  about the position  $i$  and putting  $\phi_i$  equal to  $\theta_i + \pi$ , we get for the ground-state energy,

$$H_0 = 2S^2 \sum_i [8J - a_z^2 J (\partial\theta_i / \partial z)^2 + K_1 \sin^2 \theta_i], \quad (5)$$

which, upon varying with respect to  $\theta$ , yields the useful relations, (with similar equations for  $\phi$ ),

$$\begin{aligned} (\partial\theta / \partial z)^2 &= h^2 \sin^2 \theta, \\ \cos \theta &= -\tanh(zh), \end{aligned} \quad (6)$$

where  $h = (-K_1/a_z^2 J)^{1/2}$  is the inverse of the wall thickness and  $a_z$  is the lattice distance between atoms in the  $z$  direction.

### IV. ADDITIONAL ENERGY CONTRIBUTIONS

When the Bloch wall is subject to perturbations, it will exhibit stiffness, viscosity, and inertia caused by both the interaction of the wall with the imperfections in the material and by the characteristics of the magnetic material. Unlike the ferromagnetic case, the magnetostatic energy does not play a role in the formation of domains. Nevertheless, there exist demagnetizing effects with respect to motion of the wall in the  $z$  direction, thus giving us an inertia term. As shown by Winter,<sup>3</sup> this may be represented by  $M[\sum_i (S_z^i)^2 + \sum_j (s_z^j)^2]$ . The stiffness force is essentially a structure-sensitive characteristic of the wall<sup>4</sup> and is equal to  $-\alpha(\Delta z)$ , where  $\alpha$  is the stiffness coefficient and  $\Delta z$  represents the displacement of the wall in the  $z$  direction. Following Winter,<sup>3</sup> we take account of the wall stiffness by adding to our Hamiltonian the term

$$K'[\sum_i (S_Y^i)^2 + \sum_j (s_Y^j)^2]. \quad (7)$$

Since from Eq. (6), a translation  $\Delta z$  yields the transverse components,

$$S_Y = (\Delta z)hS \sin \theta, \quad s_Y = (\Delta z)hS \sin \phi,$$

we see that this term does give a change in energy of  $\frac{1}{2}\alpha(\Delta z)^2$  where, if  $A$  is the area of the wall,

$$\alpha = 4K'h^2 S^2 A^{-1} \sum_i \sin^2 \theta_i.$$

The viscosity measures the energy losses connected with the motion of the domain wall and is thus im-

portant for relaxation time calculations. The assumption is that there is a time lag between the sudden application of a torque to change the direction of the magnetization and the time when the magnetization takes up its resultant equilibrium position.<sup>4</sup> Thus, there is a torque proportional to the time rate of change of the perturbation which resists change in the direction of the magnetization. This may be represented phenomenologically as

$$\hbar(d\mathbf{S}^i/dt)_{\text{visc}} = -\Gamma_1 S_Y^i \mathbf{e}_Y - \Gamma_2 S_z^i \mathbf{e}_z \quad (8a)$$

and

$$\hbar(ds^j/dt)_{\text{visc}} = -\Gamma_1 s_Y^j \mathbf{e}_Y - \Gamma_2 s_z^j \mathbf{e}_z, \quad (8b)$$

for perturbations  $S_Y^i$ ,  $S_z^i$  and  $s_Y^j$ ,  $s_z^j$  on the  $i$ th and  $j$ th spins.

### V. EQUATIONS OF MOTION

The equations of motion are given by the formulas

$$i\hbar d\mathbf{S}_i/dt = [\mathbf{S}_i, H], \quad (9a)$$

$$i\hbar ds_j/dt = [\mathbf{s}_j, H], \quad (9b)$$

where  $H$  is the total Hamiltonian given by Eqs. (2), (3), and (7) after placing the linear terms equal to zero by the minimization condition. [We shall add Eqs. (8) directly to Eqs. (9) to obtain complete expressions.] If, in Eq. (9a), we expand  $\mathbf{s}_j$  about the position  $i$  and in Eq. (9b), we expand  $\mathbf{S}_i$  about the position  $j$ , and only keep second-order terms in the perturbation (valid for long wavelengths), we obtain, using Eqs. (6) and the commutation relations,

$$\begin{aligned} \hbar dS_Y/dt &= -2JSa_z^2 d^2 S_z/dz^2 - 4K_1 S S_z \sin^2 \theta \\ &\quad + 2K_2 S S_z - 12JS(S_z + s_z) - \Gamma_1 S_Y + 2M S S_z \\ &\quad - 2JS(a_X^2 d^2 S_z/dX^2 + a_Y^2 d^2 S_z/dY^2), \end{aligned} \quad (10a)$$

$$\begin{aligned} \hbar ds_Y/dt &= -2JSa_z^2 d^2 S_z/dz^2 - 4K_1 S s_z \sin^2 \theta \\ &\quad + 2K_2 S s_z - 12JS(S_z + s_z) - \Gamma_1 s_Y + 2M S s_z \\ &\quad - 2JS(a_X^2 d^2 S_z/dX^2 + a_Y^2 d^2 S_z/dY^2), \end{aligned} \quad (10b)$$

$$\begin{aligned} \hbar dS_z/dt &= -2JSa_z^2 d^2 s_Y/dz^2 - 2K_1 S S_Y \cos 2\theta \\ &\quad + (S_Y - s_Y)(12JS + 2K_1 S \sin^2 \theta) \\ &\quad - 2K' S S_Y - \Gamma_2 S_z \\ &\quad - 2JS(a_X^2 d^2 s_Y/dX^2 + a_Y^2 d^2 s_Y/dY^2), \end{aligned} \quad (10c)$$

$$\begin{aligned} \hbar ds_z/dt &= -2JSa_z^2 d^2 s_Y/dz^2 - 2K_1 S s_Y \cos 2\theta \\ &\quad + (s_Y - S_Y)(12JS + 2K_1 S \sin^2 \theta) \\ &\quad - 2K' S s_Y - \Gamma_2 s_z \\ &\quad - 2JS(a_X^2 d^2 s_Y/dX^2 + a_Y^2 d^2 s_Y/dY^2). \end{aligned} \quad (10d)$$

Adding and subtracting Eqs. (10a) and (10b) and similarly for Eqs. (10c) and (10d), we obtain for the  $z$  dependence the two sets of equations

$$(\Gamma_1 + iE)\sigma_Y = -24JS\sigma_z + 2M S \sigma_z \quad (11a)$$

$$\begin{aligned} (\Gamma_2 + iE)\sigma_z &= -2JSa_z^2 (d^2 \sigma_Y/dz^2) - 2K_1 S \sigma_Y \\ &\quad \times \cos 2\theta - 2K' S \sigma_Y \\ &\quad + 2JS(a_X^2 k_X^2 + a_Y^2 k_Y^2)\sigma_Y, \end{aligned} \quad (11b)$$

and

$$(\Gamma_1 + iE)\gamma_Y = 2JSa_z^2(d^2\gamma_z/dz^2) - 4K_1S\gamma_z \sin^2\theta + 2MS\gamma_z + 2K_2S\gamma_z - 2JS(a_X^2k_X^2 + a_Y^2k_Y^2)\gamma_z, \quad (12a)$$

$$(\Gamma_2 + iE)\gamma_z = (24JS - 2K'S)\gamma_Y, \quad (12b)$$

with

$$\sigma = \mathbf{S} + \mathbf{s}, \quad \gamma = \mathbf{S} - \mathbf{s}, \quad (13)$$

where we have recognized that the anisotropy energies  $K_1$  and  $K_2$  are smaller than  $J$ , the exchange energy.

## VI. SOLUTIONS

$$\gamma = 0$$

We first consider the set of solutions  $\gamma_Y = \gamma_z = 0$ . Thus,  $S_Y = s_Y$ ,  $S_z = s_z$  and  $\sigma_Y = 2S_Y$ ,  $\sigma_z = 2S_z$ . Substituting Eq. (11a) into (11b) and placing  $u = -\cos\theta$ , we get

$$(1 - u^2) \frac{d^2\sigma_Y}{du^2} - 2u \frac{d\sigma_Y}{du} + \left[ 1(1+1) + \frac{k_z^2}{h^2} \frac{1}{1-u^2} \right] \sigma_Y = 0, \quad (14)$$

where  $k_z^2$  is given by the equation

$$\begin{aligned} E^2 - iE(\Gamma_1 + \Gamma_2) - \Gamma_1\Gamma_2 \\ = (48J^2S^2 - 4MJS^2)(a_z^2k_z^2 + a_X^2k_X^2 + a_Y^2k_Y^2) \\ - (48JS^2 - 4MS^2)(K_1 + K'). \end{aligned} \quad (15)$$

Equation (14) is the associated Legendre equation with solutions<sup>7</sup>

$$\sigma_Y = A_Y P_1^m(u) = A_Y e^{hmz} [\tanh(zh) - m] \times \exp[i(k_X X + k_Y Y)], \quad (16)$$

where  $m = \pm ik_z/h$ . For  $k_z^2/h^2 \leq 0$ , the only regular solutions with regular derivatives that can be obtained are the following:

(a)  $k_z^2/h^2 = -1$ : For this case,  $k_z$  is pure imaginary and

$$\sigma_Y = A_Y e^{-h|z|} [\tanh(zh) - 1] \exp[i(k_X X + k_Y Y)], \quad (17)$$

while  $\sigma_z$  is given by Eq. (11a). Thus, this is a bound state and does not exist outside of the wall. The energy is given by Eq. (15) with  $k_z^2 = -h^2$ . We get

$$\begin{aligned} E^2 - iE(\Gamma_1 + \Gamma_2) - \Gamma_1\Gamma_2 \\ = (-48JS^2 + 4MS^2)(K' - a_X^2k_X^2 - a_Y^2k_Y^2). \end{aligned} \quad (18)$$

Thus, for very small damping, this is a wall resonance energy of magnitude

$$\hbar\omega_0' = [(-48J + 4M)K'S^2]^{\frac{1}{2}} \quad (19)$$

at the bottom of the wall excitation branch. (Note that  $J$  is negative.) If  $K' = 0$ , then  $E = 0$  and this solution corresponds to a translation  $\Delta z$  of the Bloch wall.

<sup>7</sup> W. Magnus and F. Oberhettinger, *Special Functions of Mathematical Physics* (Chelsea Publishing Company, New York, 1949), p. 53.

(b)  $k_z^2/h^2 = 0$ : Our solution then has the form

$$\sigma_Y = -A_Y \tanh(zh) \exp[i(k_X X + k_Y Y)]. \quad (20)$$

For  $k_x = k_y = 0$ , this is the uniform mode and corresponds to the first free state. The energy is obtained by putting  $\mathbf{k} = 0$  in Eq. (15). If the wall stiffness  $K'$  is large compared to the anisotropy energy  $K_1$ , then this energy is the same as the bound-state energy given above.

(c)  $k_z^2/h^2 \geq 0$ : All the positive values of  $k_z^2/h^2$  are proper values, corresponding to solutions of the form given by Eq. (16), and form a spin-wave excitation branch. The expression for the energy is given by Eq. (15), with  $k_z = 0$  corresponding to the above-mentioned uniform mode. The lowest state occurs at an energy higher than the bottom of the wall excitation branch.

$$\sigma = 0$$

A second set of solutions is given by  $\sigma_Y = \sigma_z = 0$ . Thus,  $S_Y = -s_Y$ ,  $S_z = -s_z$  and  $\gamma_Y = 2S_Y$ ,  $\gamma_z = 2S_z$ . Substituting Eq. (12b) into Eq. (12a) and again placing  $u = -\cos\theta$ , we get an equation identical with Eq. (14) except that  $k_z^2$  is now given by the formula

$$\begin{aligned} E^2 - iE(\Gamma_1 + \Gamma_2) - \Gamma_1\Gamma_2 \\ = (48J^2S^2 - 4JK'S^2)(a_z^2k_z^2 + a_X^2k_X^2 + a_Y^2k_Y^2) \\ - 48S^2J(K_2 + M) + 4S^2K'(K_2 + M). \end{aligned} \quad (21)$$

The bound-state solution corresponding to  $k_z^2 = -h^2$  is

$$\begin{aligned} E^2 - iE(\Gamma_1 + \Gamma_2) - \Gamma_1\Gamma_2 \\ = (48JS^2 - 4K'S^2) \\ \times [K_1 - (K_2 + M) + J(a_X^2k_X^2 + a_Y^2k_Y^2)], \end{aligned} \quad (22)$$

which also yields a translation  $\Delta z$  of the Bloch wall. The energy for the uniform mode is obtained by putting  $\mathbf{k} = 0$  in Eq. (21).

If  $K'$  is greater than  $K_2 - K_1 + M$ , then this mode is lower in energy than the corresponding mode for  $S_Y = s_Y$ ,  $S_z = s_z$ , while if  $K'$  is less, then the reverse situation occurs. For  $\text{CuCl}_2 \cdot 2\text{H}_2\text{O}$ , the experimental values are  $K_1 = 5.1 \times 10^{-3} \text{ cm}^{-1}$ ,  $K_2 = 16.8 \times 10^{-3} \text{ cm}^{-1}$ , or  $K_2 - K_1$  is approximately  $2.3 \times 10^{-18} \text{ erg}$ .

The spin-wave excitation branch corresponding to positive values of  $k^2$  is given by Eq. (21). The lowest state corresponding to the uniform mode occurs at an energy higher than the bottom of the wall excitation branch.

## Degenerate Case

For simplicity, let us assume  $M = 0$ . Then we note from Eqs. (15) and (21) that, for  $K' > K_2 - K_1$ , there exist  $k_z$  states for which our two sets of solutions have equal energy values. These  $k_z$  states which we shall label  $k_z'$  are shown in Fig. (3) and correspond to the crossing of the two curves. The equation is given by (with  $k_X = k_Y = 0$ )

$$-JK'a_z^2k_z'^2 = 12J(K_2 - K_1 - K') - K_2K'. \quad (23)$$

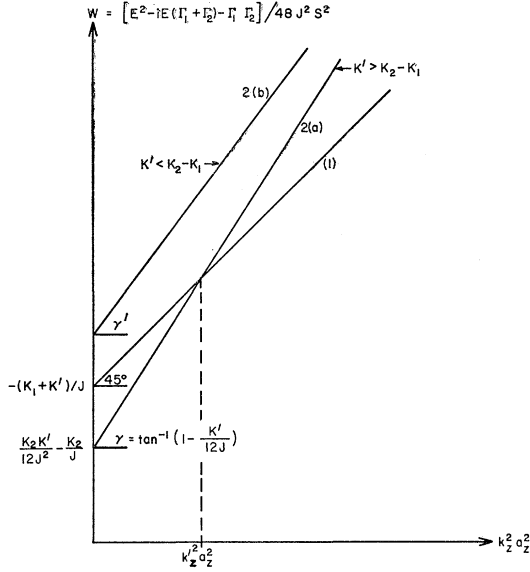


FIG. 3. Graph of energy vs wavelength. Line (1) refers to Eq. (15) and gives allowed energy values for  $S_Y = s_Y$ ,  $S_z = s_z$ . Line (2a) refers to Eq. (21) and gives allowed energy values for  $S_Y = -s_Y$ ,  $S_z = -s_z$  when the elastic energy  $K'$  is greater than  $K_2 - K_1$ , the anisotropic energy difference between the  $x$  and  $y$  directions, while line 2(b) is for  $K'$  less than  $K_2 - K_1$ . The value  $k_z'$ , occurring only for curve 2(a), corresponds to an energy degeneracy where neither of the above relations between  $\mathbf{S}$  and  $\mathbf{s}$  are necessary.

Thus, since  $k_X$  and  $k_Y$  vary independently of  $k_z'$ , there exist surfaces in  $\mathbf{k}$  space which are degenerate with respect to these two sets of solutions. Along these surfaces, neither  $\sigma$  nor  $\gamma$  need be zero and there exist more general relationships between  $S_y$  and  $s_Y$  and between  $S_z$  and  $s_z$  than those obtained previously. Using Eq. (13), we get

$$\begin{aligned} \mathbf{S} &= \frac{1}{2}(\mathbf{A} + \mathbf{B})[\tanh(zh) - ik_z'h^{-1}] \\ &\quad \times \exp[i(k_z'z + k_X X + k_Y Y)], \\ \mathbf{s} &= \frac{1}{2}(\mathbf{A} - \mathbf{B})[\tanh(zh) - ik_z'h^{-1}] \\ &\quad \times \exp[i(k_z'z + k_X X + k_Y Y)], \end{aligned} \quad (24)$$

where  $A_Y$ ,  $A_z$ ,  $B_Y$ , and  $B_z$  are the coefficients for the

wave functions  $\sigma_Y$ ,  $\sigma_z$ ,  $\gamma_Y$ , and  $\gamma_z$ , respectively. Thus, the amplitudes may now differ by a constant not equal to  $\pm 1$ . In fact, if the anisotropy were uniaxial ( $K_1 = K_2$ ) and  $K'$  was small, Eq. (24) would be the general equation for all  $k_z$ .

### Phase Changes

When crossing the Bloch wall in the sense of increasing  $z$ , Eq. (16) shows that the change of phase can be represented as

$$\beta = \tan^{-1}\{-k_z/[h \tanh(zh)]\}. \quad (25)$$

As  $z$  changes from  $-\infty$  to small  $z$  inside of the wall and then finally to  $+\infty$  on the other side of the Bloch wall, the  $\tanh(zh)$  varies from  $-1$  to  $+1$  and the phase  $\beta$  varies from  $\arctan(k_z/h)$  to  $\frac{1}{2}\pi$  to  $\arctan(-k_z/h)$ . For very small  $k_z$  or long wavelengths, this corresponds to a  $180^\circ$  phase change (from 0 to  $\pi$ ) of the spin wave—the major portion of this shift occurring within the region  $|z| < h^{-1}$ , i.e., within the Bloch wall.

For larger values of  $k_z$ , the change of phase is not a full  $\pi$  radians. For  $k_z = h$ ,  $\beta$  varies from  $\frac{1}{4}\pi$  to  $\frac{3}{4}\pi$  or a change of  $\frac{1}{2}\pi$  radians—again occurring mainly within the Bloch wall. In the limit, as  $k_z \rightarrow \infty$ , there is zero change of phase. For the uniform mode corresponding to  $k_z = 0$ , the amplitude of the spin wave goes to zero at  $z = 0$ , and then again becomes finite for  $z > 0$  but with the opposite sign.

Thus, the Bloch wall is transparent to the unbound spin-wave excitation branch whatever may be the energy of the incident wave. This is similar to the ferromagnetic case.<sup>2</sup>

### ACKNOWLEDGMENTS

The author wishes to thank Professor C. Kittel for initial discussion concerning the problem, Dr. J. Winter for the privilege of seeing his manuscript prior to publication, the U. S. Office of Naval Research for their support of this research, and the Physics Department of the University of California, Berkeley, for their hospitality during the summer months.